

Table 2.

Data	No. of data points	C_1	m	r^2	δ (%)
A: Data correlated by $Nu = C_1 Ra^n$ [equation (1)]					
All of present data	67	0.0527	0.336	0.9981	2.7
Present data less two suspect points	65	0.0548	0.335	0.9980	2.5
Present data for $Ra > 5 \times 10^8$	49	0.0492	0.339	0.9984	2.2
Present data for $Ra > 5 \times 10^8$ less two suspect points	47	0.0524	0.336	0.9988	1.9
Data of [5] plus present data less two suspect points for $Ra > 10^9$	15	0.0487	0.339	0.9988	1.7
B: Data correlated by $Nu = C_2 Ra^{1.3}$ [Equation (2)]					
		C_2	r^2	δ (%)	
All of present data	67	0.0557	0.9980	2.7	
Present data less two suspect points	65	0.0556	0.9980	2.5	
Present data for $Ra > 5 \times 10^8$	49	0.0556	0.9986	2.4	
Present data for $Ra > 5 \times 10^8$ less two suspect points	47	0.0555	0.9988	2.0	
Data of [5] plus present data less two suspect points for $Ra > 10^9$	15	0.0556	0.9986	1.9	

Suspect points of present data are at Rayleigh numbers of 1.18×10^{11} and 1.64×10^{11} ; δ is the rms deviation. r^2 is coefficient of determination for best fit of correlation.

REFERENCES

1. J. Toomre, D. O. Gough and E. H. Spiegel, Numerical solution of single-mode equations, *J. Fluid Mech.* **79**, 1 (1977).
2. R. R. Long, Relation between Nusselt number and Rayleigh number in turbulent thermal convection, *J. Fluid Mech.* **73**, 445 (1976).
3. D. C. Threlfall, Free convection in low-temperature gasoline helium, *J. Fluid Mech.* **67**, 17 (1975).
4. D. E. Fitzjarrald, An experimental study of turbulent convection in air, *J. Fluid Mech.* **73**, 693 (1976).
5. A. M. Garon and R. J. Goldstein, Velocity and heat transfer measurements in thermal convection, *Physics Fluids* **16**, 1818 (1973).
6. K. G. T. Hollands, G. D. Raithby and L. Konicek, Correlation equations for free convection heat transfer in horizontal layers of air and water, *Int. J. Heat Mass Transfer* **18**, 879 (1975).
7. I. Catton and D. K. Edwards, Effect of side walls on natural convection between horizontal plates heated from below, *J. Heat Transfer* **89**, 295 (1967).

HEAT TRANSFER CHARACTERISTICS FOR LAMINAR FLOW BETWEEN PARALLEL PLATES WITH SUCTION

L. C. CHOW

Department of Mechanical Engineering, Texas A&M University, College Station, TX 77843, U.S.A.

A. CAMPO

Universidad Simon Bolivar, Caracas, Venezuela

and

C. L. TIEN

University of California, Berkeley, CA 94720, U.S.A.

(Received 10 September 1979 and in revised form 13 December 1979)

NOMENCLATURE

D ,	half-width of the two-dimensional channel;	T ,	temperature;
l ,	nondimensional length of the channel, L/D ;	u ,	nondimensional horizontal velocity, U/U_{be} ;
L ,	length of the channel;	U ,	horizontal velocity;
Pe ,	Peclet number, $U_{be}D/\alpha$;	v ,	nondimensional vertical velocity, V/U_{be} ;
Re_e ,	inlet Reynolds number, $U_{be}D/\nu$;	V ,	vertical velocity;
Re_w ,	suction Reynolds number, $V_w/D/\nu$;	V_w ,	suction velocity, equal to $-V$ at the wall;
		x ,	nondimensional horizontal length coordinate, X/D ;

X , horizontal length coordinate;
 y , nondimensional vertical length coordinate, Y/D ;
 Y , vertical length coordinate.

Greek symbols

α , thermal diffusivity;
 θ , nondimensional temperature, $(T - T_w)/(T_{be} - T_w)$;
 ν , kinematic viscosity;
 Ψ , nondimensional stream function,
 $u = \frac{\partial \Psi}{\partial y}$ and $v = \frac{\partial \Psi}{\partial x}$;
 Ω , nondimensional vorticity, $\frac{\partial v}{\partial x} - \frac{\partial u}{\partial y}$.

Subscripts

b , bulk;
 e , inlet, $x = -2$;
 0 , at $x = 0$;
 w , wall.

INTRODUCTION

THE SUBJECT of laminar fluid flow in porous parallel-plate channels has received considerable attention over the last two decades. Applications include transpiration cooling in gas-core nuclear rockets and vapor flow in heat pipes.

Most of the early works have been restricted to determining the hydrodynamically-developed velocity profiles with uniform mass suction or injection at the walls. In these studies [1-4], the flow is assumed to be fully developed and similarity solutions are searched for from the resulting simplified equations. Berman [2] obtained the fully-developed velocity profiles for a wide range of wall Reynolds numbers for both suction and injection. In addition to the more or less parabolic-shaped fully developed velocity profile, Raithby [4] obtained a second kind of fully-developed velocity profile for cases with strong suction. This second dimensionless fully-developed velocity profile is characterized by the maximum velocity not being at the centerline, but instead skewed towards the wall with a reduced velocity at the centerline.

Raithby [4] also suggested that the final fully-developed velocity profile could depend on the inlet velocity profile. Doughty [5] has found a class of entry velocity profiles that develop quite close into this second fully-developed solution. These entry profiles are noted by a velocity defect at the channel centerline.

Raithby and Knudsen [6] solved the two-dimensional, elliptic equations of motion, with stream function and vorticity as dependent variables. They discovered that for strong suction, over the entire channel length, the velocity profile depends strongly on the inlet profile shape and, the hydrodynamically-developed solutions published previously are normally not attained nor approached by the developing flow. It therefore appears that for strong suction, fully-developed velocity profiles have little meaning and should not be used as a basis for further analysis. Gupta and Levy [7] examined the entrance region solutions by solving the two-dimensional boundary-layer equations. They assumed, in their analysis, that the inlet velocity is very large compared to the suction velocity. They also concluded that the behaviour of the flow in a channel with uniform suction at the walls is highly sensitive to both the shape of the inlet velocity profile and the value of the suction Reynolds number.

In this paper, three different inlet velocity profiles are used. The inlet velocity profile is assumed to be uniform, parabolic or double-parabolic. The uniform and parabolic velocity profiles occur quite frequently in laminar flow. The double-parabolic velocity profile, though somewhat unusual, can be obtained by inserting a thin horizontal centerplane between the parallel plates up to the region of interest. Similar to the work of Raithby and Knudsen [6], the hydrodynamic development of flow in a parallel-plate channel with wall suction is examined. The main contribution of this paper is to

study the heat-transfer characteristics when both the velocity and temperature profiles are not fully developed at the inlet. Since fully developed flows are not normally attained, the validity of the previously published heat-transfer results [4] based on fully-developed flows becomes questionable. The effects of different inlet velocity profiles on the rate of heat transfer are examined. The energy equation, including the axial conduction term, is solved simultaneously with the flow equations. Therefore, the equations in this paper are valid for ordinary fluids and liquid metals.

PROBLEM FORMULATION

The situation being considered is illustrated in Fig. 1. The flow through the channel is assumed to be steady, incompressible, laminar and two-dimensional. The channel has a width of $2D$ and length $L + 2D$, and it is open at both $X = -2D$ and $X = L$. The average axial velocity at $X = -2D$ is U_{be} . The first section of the channel ($-2D \leq X < 0$) is nonporous and thermally insulated. The rest of the channel ($0 \leq X \leq L$) is porous and the walls are kept at a uniform temperature. In this latter section, the fluid flows symmetrically out of the channel through the upper and lower porous walls with a uniform velocity, V_w . Conservation of mass requires

$$U_{be}D = V_wL. \quad (1)$$

The nonporous and insulated section of the channel allows the influence of the porous section to propagate upstream to adjust to the incoming flow, thereby avoiding the anomalous pressure and velocity behavior. It also allows the effects of heating (or cooling) at the walls downstream to penetrate upstream by axial conduction, which is especially important for liquid metals.

By introducing a non-dimensional stream function, vorticity and temperature as dependent variables, and using the following definitions,

$$u = \frac{U}{U_{be}}, \quad v = \frac{V}{U_{be}}, \quad x = \frac{X}{D}, \quad y = \frac{Y}{D}, \quad (2)$$

$$\theta = \frac{T - T_w}{T_{be} - T_w}, \quad Re_e = \frac{U_{be}D}{\nu}, \quad Pe = \frac{U_{be}D}{\alpha}$$

the governing equations for this hydrodynamic and thermal problem are:

$$\frac{\partial(u\Omega)}{\partial x} + \frac{\partial(v\Omega)}{\partial y} = \frac{1}{Re_e} \left(\frac{\partial^2 \Omega}{\partial x^2} + \frac{\partial^2 \Omega}{\partial y^2} \right), \quad (3)$$

$$\frac{\partial^2 \Psi}{\partial x^2} + \frac{\partial^2 \Psi}{\partial y^2} = -\Omega, \quad (4)$$

$$\frac{\partial(u\theta)}{\partial x} + \frac{\partial(v\theta)}{\partial y} = \frac{1}{Pe} \left(\frac{\partial^2 \theta}{\partial x^2} + \frac{\partial^2 \theta}{\partial y^2} \right) \quad (5)$$

and

$$u = \frac{\partial \Psi}{\partial y}, \quad v = -\frac{\partial \Psi}{\partial x}. \quad (6)$$

Due to symmetry, only the region between the wall ($y = 0$) and the centerline ($y = 1$) is considered.

It should be noted that the axial momentum diffusion and axial energy conduction terms are included in equations (3) and (5), respectively. To the knowledge of the writers, there are no numerical solutions reported on heat transfer for the present problem of hydrodynamic and thermal development of laminar flow through a porous parallel-plate channel with the axial conduction term included.

Since the problem is a spatially elliptic one, the values of Ψ , Ω and θ must be specified at all the boundaries. The boundary conditions for the porous section are:

for $0 \leq x \leq l$

$$y = 0: \Psi = \frac{Re_w x}{Re_e} - 1, \Omega = -\frac{\partial^2 \Psi}{\partial y^2}, \theta = 0, \quad (7a)$$

$$y = 1: \Psi = 0, \Omega = 0, \frac{\partial \theta}{\partial y} = 0, \quad (7b)$$

where $l = \frac{L}{D} = \frac{U_{be}}{V_w}$, and $Re_w = \frac{V_w D}{\nu}$.

For the nonporous and insulated section of the channel, the boundary conditions are:

for $-2 \leq x \leq 0$,

$$y = 0: \Psi = -1, \Omega = -\frac{\partial^2 \Psi}{\partial y^2}, \frac{\partial \theta}{\partial y} = 0, \quad (7c)$$

$$y = 1: \Psi = 0, \Omega = 0, \frac{\partial \theta}{\partial y} = 0. \quad (7d)$$

At the inlet of the channel ($x = -2$), the velocity profile is assumed to be uniform, parabolic or double-parabolic. The temperature profile is assumed to be uniform. Hence, the entrance boundary conditions are:

$$x = -2: \Psi = \Psi_e(y), \Omega = \Omega_e(y), \theta = 1 \quad (7e)$$

where

$\Psi_e(y) = y - 1$	uniform
$= -\frac{1}{2}y^3 + \frac{3}{2}y^2 - 1$	parabolic
$= -2y^3 + 3y^2 - 1$	double-parabolic
$\Omega_e(y) = 0$	uniform
$= 3y - 3$	parabolic
$= 12y - 6$	double-parabolic

At $x = l$, all the fluid has been extracted, and one can view $x = l$ as a plane of symmetry with the flow for $x > l$ being a mirror image of that for $x < l$. Thus, the boundary conditions at exit are:

$$x = l: \Psi = 0, \Omega = 0, \frac{\partial \theta}{\partial x} = 0. \quad (7f)$$

SOLUTION PROCEDURE

Equations (3)–(6) are solved numerically subject to the boundary conditions given by equation (7). The numerical scheme used here is due to Allen and Southwell [8]. This scheme is similar to that introduced by Raithby and Torrance [9]. In [10], the Allen–Southwell scheme was shown to have advantages over the other commonly used schemes such as the upwind-difference scheme in both accuracy and computation time. For details of the scheme used in this paper, the reader is referred to [8–10].

The vorticity at the wall ($y = 0$) is given by equation (7a, c). Chow *et al.* [11] showed that the vorticity near a wall with mass suction varies exponentially as the distance away from the wall. The new finite-difference representation for the wall vorticity developed in [11] is used here. Due to the vastly improved finite-difference representation for the wall vorticity, accurate results can be obtained with a relatively coarse grid compared to the one employed by Raithby and Knudsen [6]. In fact, the need for a fine grid in [6] is because the conventional methods for specifying the wall vorticities introduce errors that are usually significant.

Most of the results reported in this paper are obtained with 24 and 16 grid spaces in the x and y directions, respectively. By employing a finer grid for some of the computer runs, it is judged that the results given in the next section are correct to within a few per cent.

NUMERICAL RESULTS AND DISCUSSION

The main goal of the paper is to investigate the effects of different inlet velocity profiles on the heat-transfer rate. Hence, it is important to check if the present results support the conclusions of Raithby and Knudsen [6] that the flow does not tend to become fully developed for the case of strong wall suction. Three different inlet velocity profiles are used. The inlet velocity has a uniform, parabolic or double-parabolic profile. In Fig. 2, the velocity profiles, u/u_b , at various axial locations are plotted for the case of $Re_e = 300$ and $Re_w = 30$. The bulk velocity, $u_b(x)$, is given by

$$u_b(x) = \int_0^1 u dy = \begin{cases} 1 & -2 \leq x < 0 \\ 1 - x/l & 0 \leq x < l \end{cases} \quad (8)$$

It can be seen from Fig. 2 that the present results confirm the claims of Raithby and Knudsen [6]. The ranges of Re_e and Re_w tested are 150–600 and 15–60, respectively. For all the cases tested, it was observed that the flow downstream bears a strong resemblance to the inlet velocity profile. There is no tendency for the flow to develop into any of the hydrodynamically developed solutions. For the case of double-parabolic inlet velocity profile, one interesting observation is that the flow downstream tends to become more and more skewed towards the wall (see Fig. 2). In fact, at $x \approx 0.9l$, the axial velocity near the centerline becomes negative. However, this kind of recirculation phenomenon seems to occur only when the wall suction rate is high ($Re_w \geq 30$) and the duct length is fairly long ($l \geq 9$).

To demonstrate the importance of the inlet velocity profile on the heat transfer rate, the bulk temperature, θ_b , is plotted vs x in Fig. 3 for different inlet velocity profiles. The bulk temperature is defined as,

$$\theta_b(x) = \frac{1}{u_b} \int_0^1 u \theta dy. \quad (9)$$

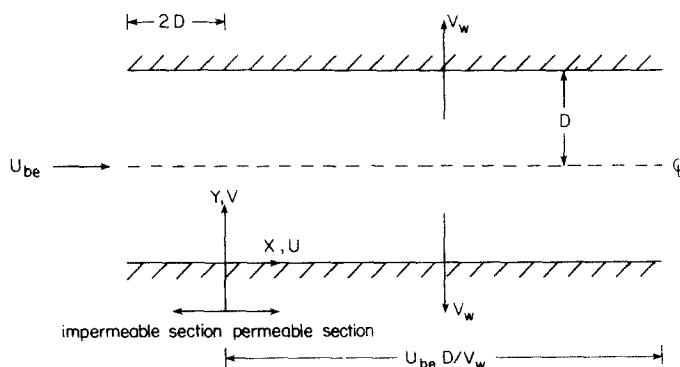


FIG. 1. Geometry and coordinate system.

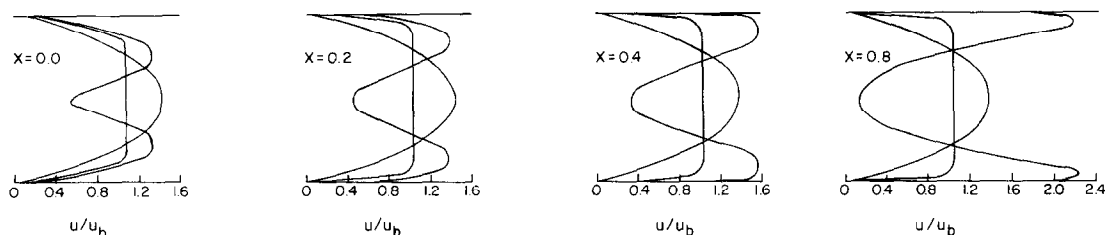


FIG. 2. Velocity profiles at various axial locations, $Re_e = 300$, $Re_w = 30$.

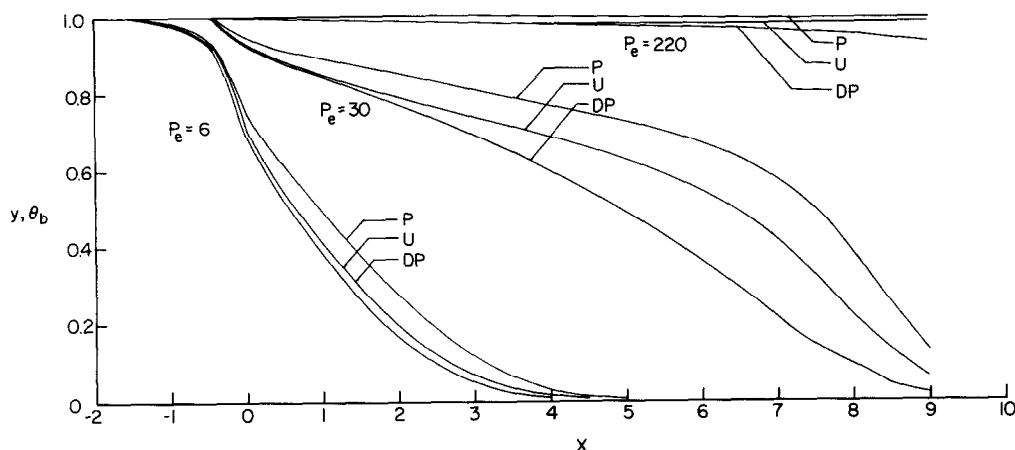


FIG. 3. Bulk temperature for different inlet velocity profiles and Peclet numbers.

It is not surprising that θ_b depends on the inlet velocity profiles, especially when the Peclet number is low. By observing Fig. 3, three points should be noted. For $Pe = 30$, in the mid-region of the channel, the bulk temperature with a double-parabolic velocity profile is only about 60% of that with a parabolic velocity profile. Hence, the usefulness and validity of previously published results on heat transfer for the present problem without considering the inlet velocity profile are questionable.

The second point is, for the wide range of Peclet numbers tested, the bulk temperature is consistently highest for flow with a parabolic inlet velocity profile, followed by flow with a uniform inlet velocity profile, and then flow with a double-parabolic inlet velocity profile. The reason is evident by observing the velocity profiles in Fig. 2. The fluid velocity near the wall is highest for flow with a double-parabolic inlet velocity profile compared to the other two cases. Thus, for the double-parabolic case, it is expected that heat transfer is more efficient, resulting in the lowest bulk temperature.

The third point that can be made by observing Fig. 3 is that the bulk temperature at $x = 0$ (where heating and cooling begins) is not unity due to the axial heat conduction. This effect is particularly important for liquid metals. For example, for $Pe = 6$, 30% of the heat transfer has already occurred before the fluid even reaches the heating (or cooling) section. At low Peclet numbers, the upstream penetration of energy by the axial conduction is important. Neglecting the axial conduction term in equation (5) may lead to substantial errors.

REFERENCES

1. A. S. Berman, Laminar flow in channels with porous walls, *J. Appl. Phys.* **24**, 1232-1235 (1953).
2. A. S. Berman, Effects of porous boundaries on the flow of fluids in systems with various geometries, *Proceedings of Second United Nations International Conference on Peaceful Uses of Atomic Energy, Geneva* **4**, 351-358 (1958).
3. S. W. Yuan, Further investigation of laminar flow in channels with porous walls, *J. Appl. Phys.* **27**, 267-269 (1956).
4. G. D. Raithby, Laminar heat transfer in the thermal entrance region of circular tubes and two-dimensional rectangular ducts with wall suction and injection, *Int. J. Heat Mass Transfer* **14**, 223-243 (1971).
5. J. R. Doughty, Parallel porous plate channel flow characteristics resulting from nonuniform entry velocity profiles, *J. Fluids Engng* **97**, 78-81 (1975).
6. G. D. Raithby and D. C. Knudsen, Hydrodynamic development in a duct with suction and blowing, *J. Appl. Mech.* **41**, 892-902 (1974).
7. B. K. Gupta and E. K. Levy, Symmetrical laminar channel flow with wall suction, *J. Fluids Engng* **98**, 469-475 (1976).
8. D. N. de G. Allen and R. V. Southwell, Relaxation methods applied to determine the motion, in two dimensions, of a viscous fluid past a fixed cylinder, *Q. J. Mech. Appl. Math.* **8**, 129-145 (1955).
9. G. D. Raithby and K. E. Torrance, Upstream-weighted differencing schemes and their application to elliptic problems involving fluid flow, *Comp. Fluids* **2**, 191-206 (1974).
10. L. C. Chow and C. L. Tien, An examination of four differencing schemes for some elliptic-type convection equations, *Num. Heat Transfer* **1**, 87-100 (1978).
11. L. C. Chow, Y. K. Cheung and C. L. Tien, A new finite-difference representation for the vorticity at a wall with suction, *Num. Heat Transfer* **1**, 417-423 (1978).